

SOME REMARKS ON A MATHEMATICAL MODEL FOR WATER FLOW IN POROUS MEDIA WITH COMPETITION BETWEEN TRANSPORT AND DIFFUSION

JUDITA RUNCZIKOVÁ*, JAN CHLEBOUN, CHIARA GAVIOLI, PAVEL KREJČÍ

Czech Technical University in Prague, Faculty of Civil Engineering, Department of Mathematics, Thákurova 7, 166 29 Prague 6 – Dejvice, Czech Republic

* corresponding author: judita.runczikova@fsv.cvut.cz

ABSTRACT. The contribution deals with the mathematical modelling of fluid flow in porous media, in particular water flow in soils. The motivation is to describe the competition between gravity and capillarity, or, in other words, between transport and diffusion. The analysis is based on a mathematical model developed by B. Detmann, C. Gavioli, and P. Krejčí, in which the effects of gravity are included in a novel way. The model consists of a nonlinear partial differential equation describing both the gravitational transport and the capillary diffusion of water. Although analytical solutions can be obtained for some special cases, only numerical solutions are available in more general situations. The solving algorithm is based on a time discretisation and the finite element method, and is written in Matlab. The results of the numerical simulations are shown and the behaviour of the model is discussed.

KEYWORDS: porous media, water flow, transport, diffusion, PDE, numerical methods.

1. INTRODUCTION

Mathematical models for water flow in unsaturated porous media, such as soils, play an important role in many applications. They have proven to be useful in geoscience and environmental engineering (e.g. spreading of contamination into soil and groundwater, and their sanitation), in civil engineering (e.g. the effect of water content on structures), and in other industrial applications.

A simple mathematical model for water flow in saturated porous media is obtained from the mass balance equation (i.e. the continuity equation) combined with the Darcy law for the water mass flux. If the porous media is unsaturated, the water flux is described by a saturation-dependent variant of the Darcy law (also called the Darcy-Buckingham law), and the resulting equation is known as the Richards equation [1]. Many numerical methods have been used to solve the Richards equation. Some of them, with their advantages and limitations, are studied for example in [2–5].

More elaborate mathematical models accounting for additional effects can be found in the literature. An occurrence of preferential flow (i.e. preferential paths through which water flows more easily) is solved for example in [6]. In [7], the Richards equation with hysteresis is introduced. Finger flow and the effects of capillary hysteresis in the model are the objects of [8].

This paper is structured as follows. In Section 2, the partial differential equation (PDE) that models unsaturated fluid flow in a porous medium is presented, and the solving algorithm is described. In Section 3, the results of numerical simulations are shown and

discussed. Examples with different initial and boundary conditions related to elementary hydrological processes in a soil column are considered in this paper.

2. MATERIALS AND METHODS

2.1. THE MATHEMATICAL MODEL

A mathematical model was proposed by Bettina Detmann, Chiara Gavioli, and Pavel Krejčí [9] with the aim of describing the fluid flow in an unsaturated porous medium under both gravitational transport and capillary diffusion. Its main feature is a "stickiness" condition: if the saturation stays below a certain threshold \bar{s} , no transport takes place, and water flows only by diffusion. This behaviour is encoded in the positive part in (1) below.

The model is a good approximation of the real behaviour when s stays away from the (expected) maximum value 1. The passage to the full saturation case can be included, too, by cutting off from above the nonlinearity in (1) to take into account the entrapped air. This will be the subject of future research.

The mathematical model derived from the mass balance equation is the following:

$$s_t - \kappa \Delta p - 2\alpha g (s - \bar{s})^+ s_z = 0, \quad (1)$$

where $s = s(\mathbf{x}, t) \in (0, 1)$ is the saturation (i.e. the ratio between the water volume and pore volume), s_t its time derivative, s_z its derivative with respect to z (i.e. the variable representing the vertical direction), and p is the capillary pressure. The notation $(\cdot)^+$ represents the nonnegative part of a function. The time is denoted by $t \geq 0$, the porous body is represented by a domain $\Omega \subset \mathbb{R}^3$ with coordinates $\mathbf{x} = (x, y, z) \in \Omega$ and with Lipschitz boundary $\partial\Omega$. The parameter κ is

the diffusion coefficient, α is the characteristic time related to the friction on the liquid-solid interface, g is the gravity constant, and $\bar{s} \in (0, 1)$ denotes a residual saturation value. If $s \leq \bar{s}$, then s can increase or decrease only due to the flow driven by diffusion. The model is complemented by a constitutive relation between the saturation s and the capillary pressure p . Experimental evidence indicates that the dependence is of hysteresis type, but only linear dependence is considered in this paper.

The model in [9] is also coupled with an initial condition

$$s(\mathbf{x}, 0) = s_0(\mathbf{x}) \quad (2)$$

and boundary conditions assuming no flow through the vertical parts of the boundary

$$Q \cdot n = 0, \quad (3)$$

where Q is the water mass flux vector, n the unit outward normal vector, and \cdot denotes the scalar product. The model is completed by boundary conditions prescribing the inflow/outflow through the horizontal parts of the boundary

$$Q \cdot n = \beta(s - s_{out}), \quad (4)$$

where β depends on the permeability coefficient and s_{out} is an outer concentration. In what follows, other boundary conditions on the horizontal part of the boundary will also be taken into account for this model, including the Dirichlet type for its numerical simplicity.

The model equation, the initial condition, and the boundary conditions for the 1-D flow are listed in Section 2.2. More details can be found in [9].

2.2. ALGORITHM

The vertical flow of water through a column of soil is modelled as 1-D flow through an unsaturated porous body. Transport and diffusion effects are taken into account. The relation between pressure and saturation is chosen to be linear, that is,

$$s = \gamma p, \quad (5)$$

where $\gamma = 1$.

Equation (1) in the 1-D case coupled with relation (5) reduces to

$$s_t - \kappa s_{zz} - 2\alpha g (s - \bar{s})^+ s_z = 0, \quad (6)$$

where $\kappa > 0$, $\alpha > 0$, $g > 0$, and $\bar{s} \in (0, 1)$ are constants. The domain is defined as $\Omega = (-h, 0)$ with coordinate $z \in (-h, 0)$, so that $s = s(z, t)$ and $p = p(z, t)$.

The equation-solving algorithm, based on the finite element method, is developed in Matlab. First, parameter values, time interval, and spatial mesh (vector of chosen points) are set up, as well as the initial and boundary conditions. Then, the `pdepe` procedure

(namely, the solver for systems of parabolic and elliptic PDEs of one spatial variable x and time t) is used. The options of the solver are set up as default, except the relative error tolerance ('`RelTol`') which in the examples in Section 3 is set equal to 10^{-5} . The domain is discretised by fixed division points. The time mesh is set up automatically, because the time is discretised by the `ode15s` solver. This multistep solver is a variable-step, variable-order solver based on the numerical differentiation formulas of orders 1 to 5 [?]. More details about the `pdepe` solver can be found in [10]. Then, the graphical outputs are generated.

The initial condition (i.e. the saturation at the initial time $t = 0$) is defined for all $z \in (-h, 0)$ as

$$s(z, 0) = s_0(z), \quad (7)$$

where s_0 is a given function in $L^2(-h, 0)$ taking values between 0 and 1.

The boundary conditions (BC) can be defined for $z = -h, 0$ and $t > 0$ as

- given values on the boundary (Dirichlet BC)

$$s(0, t) = f_+(t), \quad s(-h, t) = f_-(t); \quad (8)$$

- given mass flux through the boundary (Neumann BC)

$$\kappa s_z + \alpha g [(s - \bar{s})^+]^2 = \begin{cases} f_+ & \text{for } z = 0, \\ f_- & \text{for } z = -h; \end{cases} \quad (9)$$

- mass flux proportional to inner/outer saturation difference (Newton BC)

$$\kappa s_z + \alpha g [(s - \bar{s})^+]^2 = \begin{cases} -\beta_+(s - s_+) & \text{for } z = 0, \\ \beta_-(s - s_-) & \text{for } z = -h; \end{cases} \quad (10)$$

where f_+, f_- are given time dependent functions, $\beta_+ > 0, \beta_- > 0$ are the permeability coefficients of the top and of the bottom, respectively, and $s_+, s_- \in [0, 1]$ are the values of the outer saturation. BC as in (8) with $f_+ = f_- = 0$ is considered in Section 3.3, BC as in (9) with $f_+ = f_- = 0$ is considered in Section 3.1 and Section 3.2.

The validity of the mass conservation is monitored by computing the definite integral of the solution s over the domain by trapezoidal numerical integration. In the case of no inflow/outflow, the value of the integral has to remain constant over time. In the other cases, the value of the integral should comply with the difference between the inflow and outflow of water over the boundary. Thus, the water mass balance can be checked during the execution of the Matlab program.

3. RESULTS

An instance of redistribution after infiltration is introduced as an example in Section 3.1. The resulting

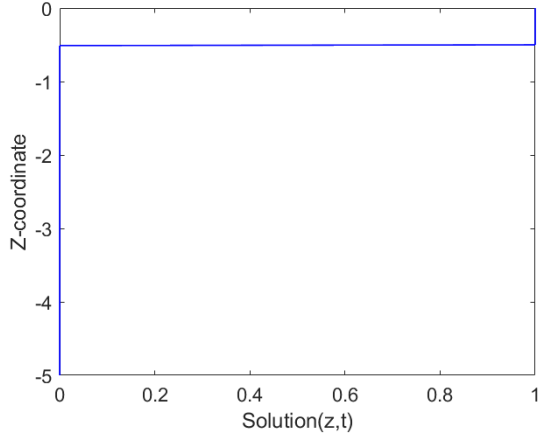


FIGURE 1. Initial condition (11).

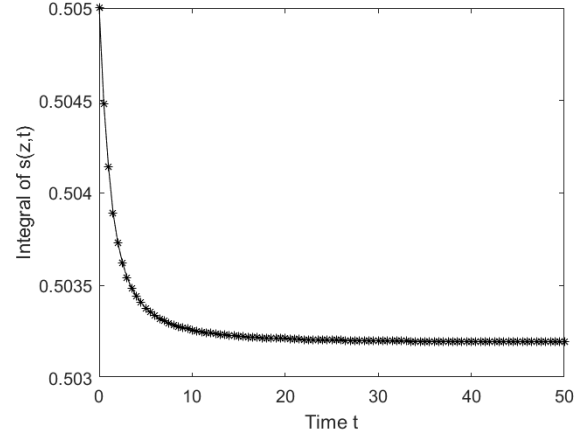


FIGURE 2. Integral of the solution over the domain.

saturation profiles are in agreement with the results for this elementary hydrological process from [11]. This redistribution phenomena is also mentioned in [12], where hysteresis effects are additionally included. The initial condition corresponds to saturated soil in a layer of given thickness below the terrain with a steep transition (almost a jump) to dry soil. In Section 3.2, the process of wetting the soil column with a water source located in the bottom layer of the column is examined. In Section 3.3, the impact of κ and \bar{s} on a similar setting is studied.

Sandy loam is considered in the following examples, with residual volumetric water content $\theta_r = 0.111$ and volumetric water content of the saturated medium $\theta_s = 0.482$, which is in turn equal to the porosity n_{por} . Thus, $\bar{s} = \theta_r/n_{por} = 0.111/0.482 = 0.2303$.

3.1. EXAMPLE 1

In this first example the parameters are chosen as follows: diffusion coefficient $\kappa = 0.005$, $2\alpha g = 1$, maximal depth $h = 5$, value of the space discretization parameter $d = 0.01$. The value of the time step τ is chosen automatically by the solver. The initial condition (displayed in Figure 1) is chosen as

$$s_0(z) = \begin{cases} 1 & \text{for } z > -0.50, \\ 100z + 51 & \text{for } z = [-0.51, -0.50], \\ 0 & \text{for } z < -0.51, \end{cases} \quad (11)$$

which means saturated soil to the depth of 0.5 and dry soil below. The BC is that of impermeable boundary

$$\kappa s_z + \alpha g [(s - \bar{s})^+]^2 = 0, \quad (12)$$

so that the control integral of the saturation over the domain remains constant over time, as displayed in Figure 2. The exception is the small interval (of order 10^{-4}) at the beginning, caused by a sharp change in the shape of the saturation curve.

The saturation profile at selected times $t = 0.5, 5, 250, 2500$ is plotted in Figure 8. At the beginning of the redistribution process, a rapid change

in the saturation profile in the upper layer can be noticed. A significant shift of the water content from the upper to the lower layer is then observed, that is, the water content decreases in the upper layer (above the wetting front) and increases in the lower layer. The terrain saturation decreases from $s = 1$ to near $s = \bar{s}$. This is caused by the dominant effect of transport in this zone. The effect of diffusion (note that κ has a significantly large value) can be seen on the shape of the wetting front, which is slowly tilting and moving downward.

The saturation value over time decreases close to the terrain and increases in the lower layers. According to (6), if the value $s(z_i, t)$ of the saturation at a given depth z_i is smaller than \bar{s} , then the transport term is not active at z_i , and the water movement is driven only by diffusion. Hence, if the saturation in the upper layers decreases until it reaches the value \bar{s} , then only the diffusion term contributes to the redistribution of water. With the above parameter setting, the saturation along the entire soil column drops below \bar{s} at time $t = 152$, as can be seen in Figure 3. The water is then redistributed by diffusion until it reaches a uniform distribution profile along the soil column, and the maximal value of s decreases until it meets the minimal value, as shown in Figure 3. From time $t = 1756$, the difference between the maximum and minimum value of the solution is less than 0.1. The process slows down as the saturation value decreases.

3.2. EXAMPLE 2

The initial condition is now changed to

$$s_0(z) = \begin{cases} 0 & \text{for } z > -4.50, \\ -30z - 135 & \text{for } z = [-4.50, -4.51], \\ 0.3 & \text{for } z < -4.51, \end{cases} \quad (13)$$

which means unsaturated soil with saturation equal to $s = 0.3$ (hence $s > \bar{s}$) in a bottom layer of thickness equal to 0.49 with a steep transition to dry soil up to terrain. The other parameters and boundary conditions are as above. The saturation profile at selected

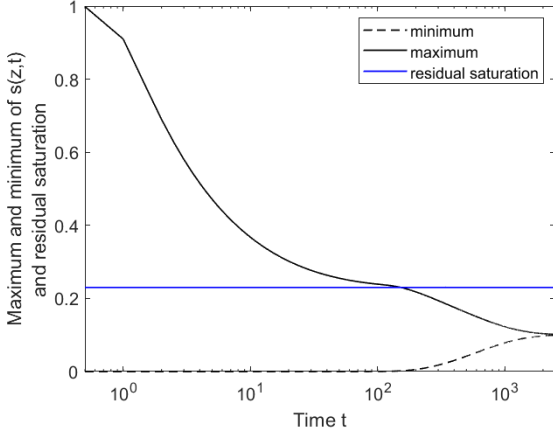


FIGURE 3. Maximum and minimum of the solution $s(z, t)$ in the range defined by the time steps and residual saturation.

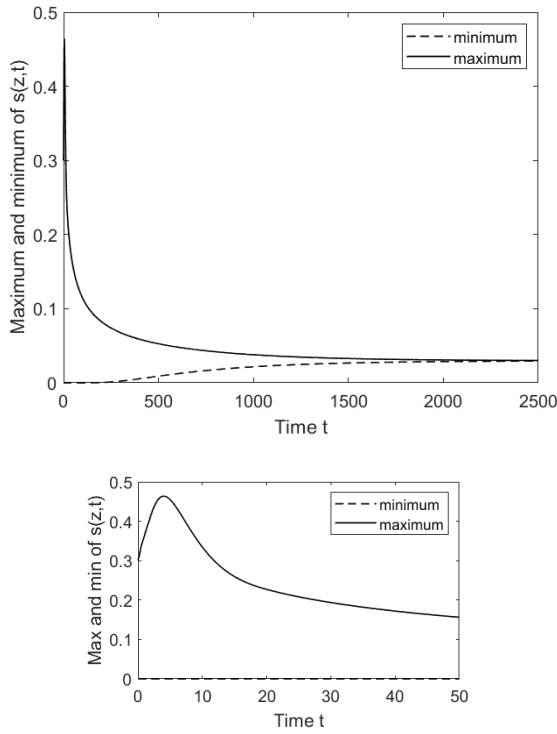


FIGURE 4. Maximum and minimum of the solution $s(z, t)$ in the range defined by the time steps (top) and zoom to the beginning of the calculation (bottom).

times $t = 0.5, 5, 250, 2500$ is plotted in Figure 9. First, flow driven by transport near the bottom and by diffusion above the unsaturated layer is observed. Then the transport-driven flow in the lower layers becomes weaker, the saturation starts to decrease and when the threshold value \bar{s} is met, the transport term becomes inactive, so that only the upper layers are continuously wetted by diffusion. The profiles of maximal and minimal soil saturation over time are shown in Figure 4, where the peak in the bottom figure occurs at the time when the increase in saturation due to transport in the lower layer ends.

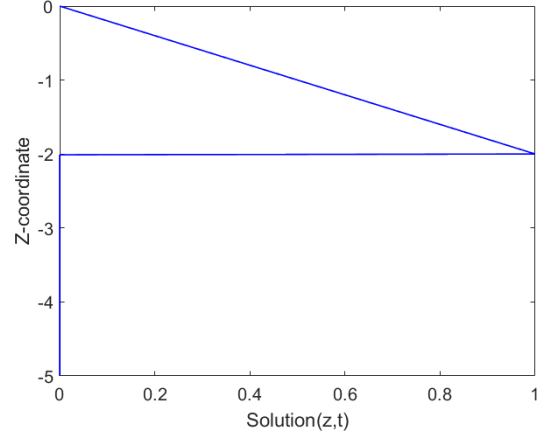


FIGURE 5. Initial condition (14) with a steep wetting front.

3.3. EXAMPLE 3

The influence of the choice of κ and \bar{s} on the saturation profile is shown in the next examples. The following parameters are chosen: $\gamma = 1$, $2\alpha g = 1$, diffusion coefficient κ in the range $[0, 0.01]$, residual saturation $\bar{s} = 0$ or $\bar{s} = 0.2303$, maximal depth $h = 5$, value of the space discretization parameter $d = 0.01$. The value of the time step τ is chosen automatically by the solver. The initial condition is now chosen as

$$s_0(z) = \begin{cases} -0.5z & \text{for } z > -2.00, \\ 100z + 201 & \text{for } z = [-2.00, -2.01], \\ 0 & \text{for } z < -2.01, \end{cases} \quad (14)$$

and is displayed in Figure 5. For numerical simplicity, the boundary condition here is of Dirichlet type (8) with $f_+ = f_- = 0$.

The diffusion-driven flow is determined by the value of the diffusion coefficient κ . If $\kappa = 0$, the diffusion term in (6) is inactive. If the value of κ is close to 0, for example $\kappa = 0.001$, the diffusion is negligible. Higher values of κ are associated with strong diffusion.

If the diffusion is strong enough, that is, the value of κ is large enough, it is possible to choose an initial condition with a steep transition between two different saturation values, because the gradient of the solution soon becomes slightly smaller during the calculation due to the diffusion flow, and the simulation is stable. This situation occurs in this example in Figure 6, bottom, and also in Sections 3.1 and 3.2. Conversely, when the value of κ is small, the gradient of the solution remains large, or even tends to infinity, and numerical instabilities (i.e. oscillations of the solution) occur. Depending on the value of κ , these oscillations can cause calculation collapse, as shown in Figure 6, top, or disappear, as in Figure 6, centre.

The same analysis applies if a high saturation gradient between the wet and dry parts of the porous body occurs later in the calculation.

In Figure 7 the effect of the residual saturation \bar{s} on the solution s is shown. When \bar{s} is higher, the wetting front reaches a smaller depth.

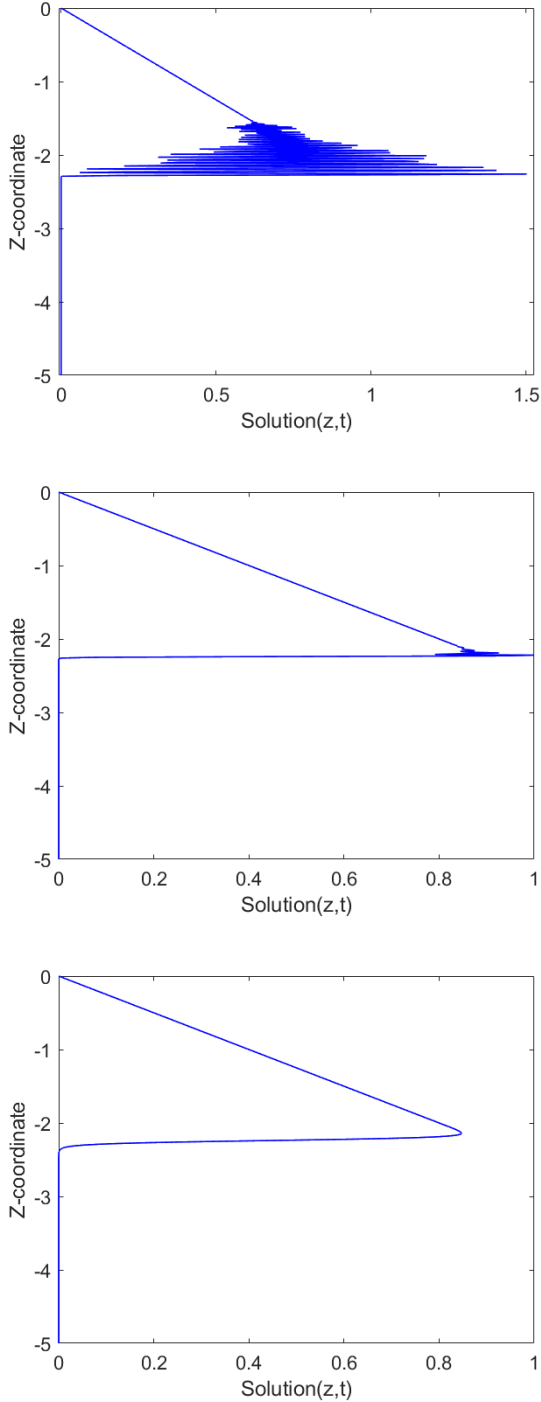


FIGURE 6. Effect of the diffusion coefficient κ on the solution $s(z, 0.5)$: without diffusion ($\kappa = 0$, top), negligible diffusion ($\kappa = 0.001$, centre), and strong diffusion ($\kappa = 0.01$, bottom).

4. CONCLUSIONS

A mathematical model for the unsaturated flow of water in a porous medium was studied. Numerical simulations of a vertical 1-D water flow in an unsaturated soil column were performed. The case of redistribution of water in soil after infiltration was shown, and the results were compared with theoretical physical expectations from the technical literature.

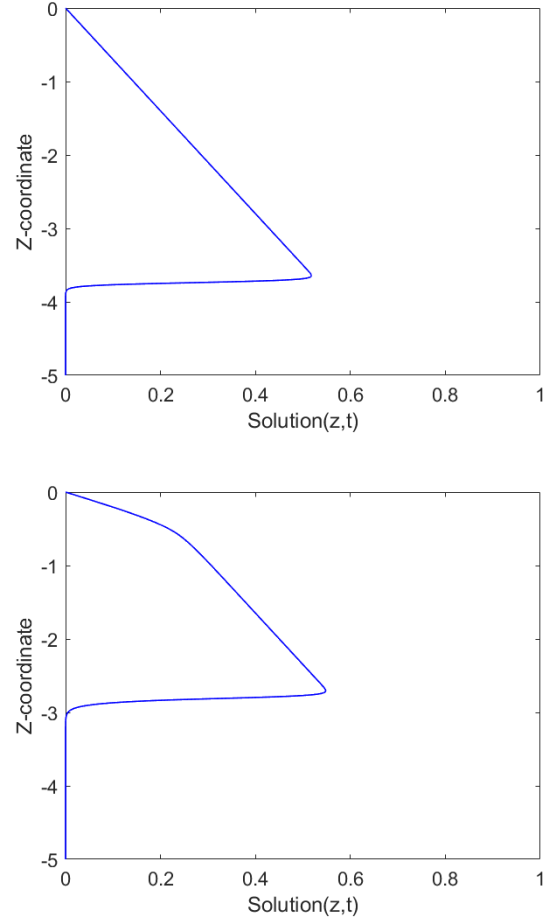


FIGURE 7. Effect of \bar{s} on the solution $s(z, 5)$ with $\kappa = 0.005$: without stickiness ($\bar{s} = 0$, top) and with stickiness ($\bar{s} = 0.2303$, bottom).

The case of infiltration from below was also considered. The model has shown a good approximation of the physical behaviour because, with the no-flux boundary condition (12), the saturation values stay under control even if we initially allow $s = 1$ in a layer of given thickness as in (11).

The effect of two parameters, the permeability κ and the residual saturation \bar{s} , was studied. Their magnitude has a significant impact on the solution, and in some cases on the stability of the calculation.

From the modelling point of view, the continuation of this research will include the case when the saturation s becomes close to 1. From the numerical point of view, future investigations will be directed towards the development of an algorithm for the 2-D flow, to test the behaviour of the model in 2-D ($\Omega \subset \mathbb{R}^2$). The influence of hysteresis and the preferential flow should also be explored.

LIST OF SYMBOLS

- s Saturation
- p Capillary pressure
- κ Diffusion coefficient
- \bar{s} Residual saturation

- α Characteristic time
 g Gravity constant

ACKNOWLEDGEMENTS

Supported by the project Centre of Advanced Applied Sciences (CAAS) No. CZ.02.1.01/0.0/0.0/16 019/0000778, which is co-financed by the European Union; by the Grant Agency of the Czech Technical University in Prague, grant No. SGS23/092/OHK1/2T/11; by the European Union's Horizon 2020 research and innovation programme under the Marie Skłodowska-Curie grant agreement No 101102708; by the Czech Ministry of Education, Youth and Sports (MŠMT) grants 8J23AT008 and 8X23001; by the Czech Science Foundation (GAČR), project No. 24-10586S.

REFERENCES

- [1] Černý, R., Rovnaníková, P. *Transport Processes in Concrete*. Spon Press, London, 2002. ISBN 0-415-24264-9.
- [2] Haverkamp, R., Vauclin, M. A comparative study of three forms of the richard equation used for predicting one-dimensional infiltration in unsaturated soil. *Soil Science Society of America Journal* **45**:13–20, 1981. <https://doi.org/10.2136/sssaj1981.03615995004500010003x>
- [3] Ross, P. J. Efficient numerical methods for infiltration using richards' equation. *Water Resour Res* **26**(2):279–290, 1990. <https://doi.org/10.1029/WR026i002p00279>
- [4] List, F., Radu, F.A. A study on iterative methods for solving richards' equation. *Comput Geosci* **20**:341–353, 2016. <https://doi.org/10.1007/s10596-016-9566-3>
- [5] Farthing, M.W., Ogden, F.L. Numerical solution of richards' equation: A review of advances and challenges. *Soil Science Society of America Journal* **81**:1257–1269, 2017. <https://doi.org/10.2136/sssaj2017.02.0058>
- [6] Vogel, T., Březina, J., Dohnal, M., Dušek, J. Physical and numerical coupling in dual-continuum modeling of preferential flow. *VADOSE ZONE JOURNAL* **9**, 2010. <https://doi.org/260-267.10.2136/vzj2009.0091>
- [7] Schweizer, B. Instability of gravity wetting fronts for richards equations with hysteresis. *Interfaces and Free Boundaries* **14**:37–64, 2012. <https://doi.org/10.4171/IFB/273>
- [8] Roche, W.J., Murphy, K., Flynn, D.P. Modelling preferential flow through unsaturated porous media with the preisach model and an extended richards equation to capture hysteresis and relaxation behaviour. *Journal of Physics: Conference Series* **1730**(012002), 2021. <https://doi.org/10.1088/1742-6596/1730/1/012002>
- [9] Detmann, B., Gavioli, C., Krejčí, P. Soil moisture transport and diffusion driven by gravity and capillarity. [in preparation].
- [10] Skeel, R. D., Berzins, M. A method for the spatial discretization of parabolic equations in one space variable. *SIAM Journal on Scientific and Statistical Computing* **11**:1–32, 1990.
- [11] Kutílek, M., Kuráž, V., Císlerová, M. *Hydropedologie 10. 2. přeprac. vydání*. ČVUT v Praze, Praha, 2000. ISBN 80-01-02237-4.
- [12] Youngs, E.G. Application of scaling to soil-water movement considering hysteresis. In *Scaling in Soil Physics: Principles and Applications*, chap. 3. John Wiley & Sons, Ltd, 1990.

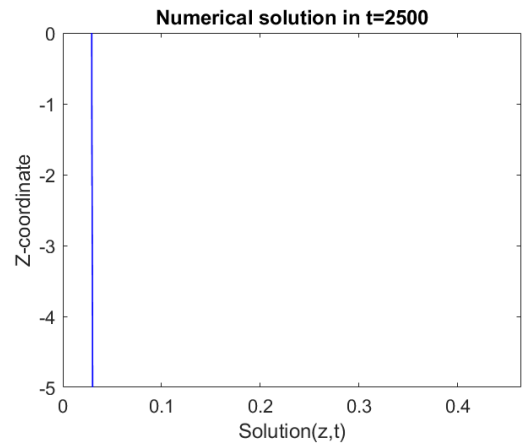
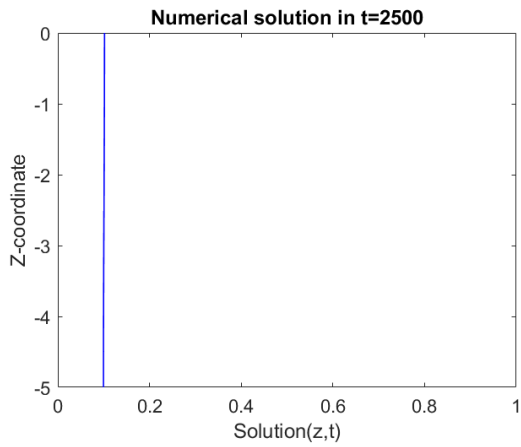
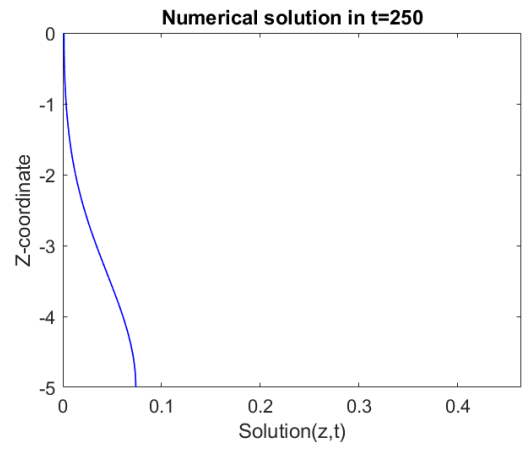
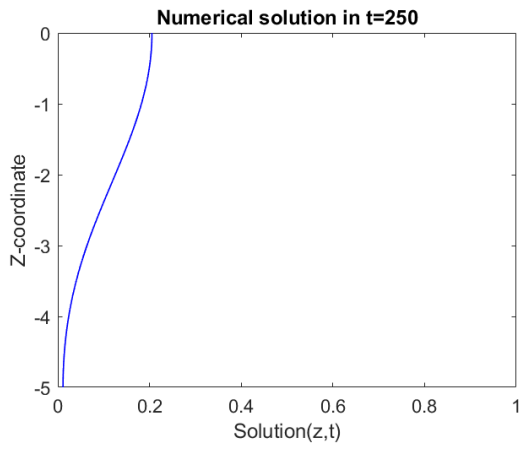
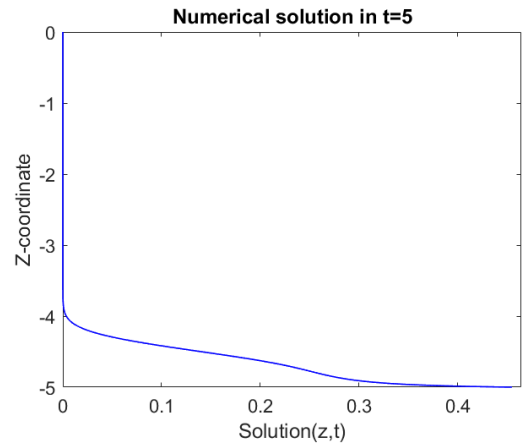
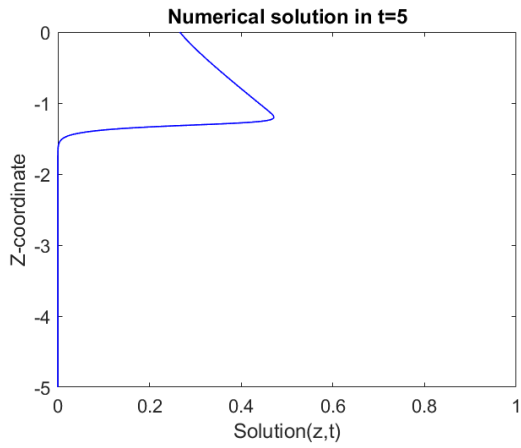
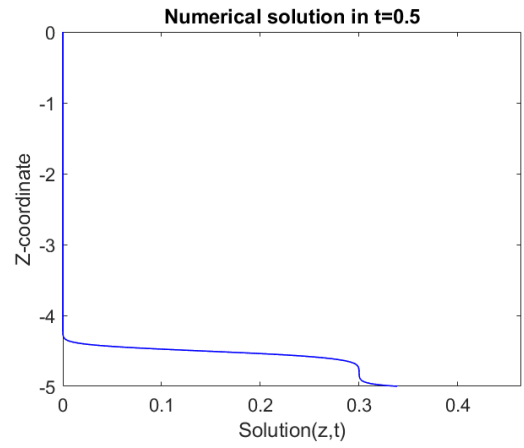
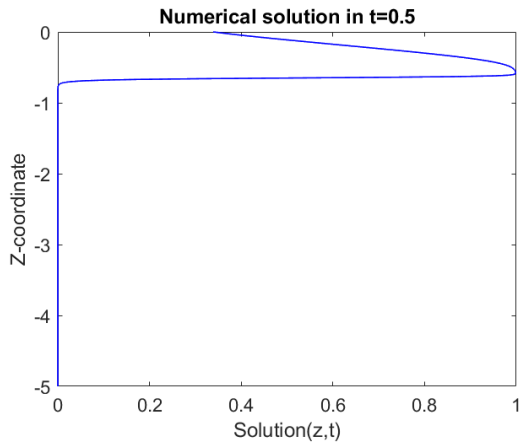


FIGURE 8. Evolution of the solution $s(z, t)$ over time with $\kappa = 0.005$ and initial condition as in (11).

FIGURE 9. Evolution of the solution $s(z, t)$ over time with $\kappa = 0.005$ and initial condition as in (13).